Horst Tobias Witt

Photosynthesis Research **80:** 85–107, 2004.

Personal perspective

Steps on the way to building blocks, topologies, crystals and X-ray structural analysis of Photosystems I and II of water-oxidizing photosynthesis

Horst Tobias Witt
Technische Universität Berlin, Max-Volmer-Laboratorium für Biophysikalische Chemie, Strasse des 17. Juni 135, 10623 Berlin, Germany (e-mail: witt@phosis1.chem.tu-berlin.de; fax: +49-30-31421122)

Received 4 April 2003; accepted in revised form 12 December 2003

Key words: antenna systems, J. Barber, E.J. Boekema, K. Brettel, crystals, cyanobacteria, J.P. Dekker, B. Diner, G. Döring, electron transfer, P. Fromme, W. Junge, N. Krauß, H. Kretschmann, W. Kühlbrand, P. Orth, Photosystem I, Photosystem II, R. Reich, G. Renger, R.H. Rhee, M. Rögner, B. Rumberg, H. Rüppel, B. Rutherford, W. Saenger, Ö. Saygin, G.H. Schatz, E. Schlodder, W.D. Schubert, H.H. Stiehl, structure, H.T. Witt, I. Witt, Ch. Wolff, X-ray crystallography, A. Zuoni

Abstract

Basic structural elements of the two photosystems and their component electron donors, acceptors, and carriers were revealed by newly developed spectroscopic methods in the 1960s and subsequent years. The spatial organization of these constituents within the functional membrane was elucidated by electrochromic band shift analysis, whereby the membrane-spanning chlorophyll–quinone couple of Photosystem (PS) II emerged as reaction center and as a model relevant also to other photosystems. A further step ahead for improved structural information was realized with the use of thermophilic cyanobacteria instead of plants which led to isolation of supramolecular complexes of the photosystems and their identification as PS I trimers and PS II dimers. The preparation of crystals of the PS I trimer, started in the late 1980s. Genes encoding the 11 subunits of PS I from *Synechococcus elongatus* were isolated and the predicted sequences of amino acid residues formed a basis for the interpretation of X-ray structure analysis of the PS I crystals. The crystallization of PS I was optimized by introduction of the 'reverse of salting in' crystallization with water as precipitating agent. On this basis the PS I structure was successively established from 6 Å resolution in the early 1990s up to a model at 2.5 Å resolution in 2001. The first crystals of the PS II dimer, capable of water oxidation, were prepared in the late 1990s; a PS II model at 3.8–3.6 Å resolution was presented in 2001. Implications of the PS II structure for the mechanism of transmembrane charge separation are discussed. With the availability of PS I and PS II crystals, new directional structural results became possible also by application of different magnetic resonance techniques through measurements on single crystals in different orientations.

Abbreviations: BChl – bacteriochlorophyll; Bpheo – bacteriopheophytin; Car – carotenoid; Chl – chlorophyll; CP43,47 – inner antenna system of PS II, with Mr of 43 and 47 kDa; Cyt – cytochrome; D1 – D1 subunit of the PS II reaction center; D2 – D2 subunit of the PS II reaction center; ENDOR – electron nuclear double resonance; EPR – electron paramagnetic resonance; ETC – electron transfer chain; EXAFS – extended X-ray absorption fine structure; $P_{D1/D2}$ – Chl coordinated by His 198/197 of D1/D2; Pheo – pheophytin; P680 – primary electron donor of PS II; P700 – primary electron donor of PS I; Q – plastoquinone of a pool; Q_A – stable primary quinone acceptor of PS II RC; RC – reaction center; Y_D – Tyr 160 of D2; Y_Z – Tyr 161 of D1

Two distinct photosystems working in series – the tandem driving water-oxidizing photosynthesis

With its conversion of light energy of the sun into biochemical energy and the supply of oxygen from water for the biosphere, oxygenic photosynthesis is the very basis of life on our planet. Nature has invented different, unique mechanisms for realizing this process. One of these was the coupling of two different Photosystems I and II working in series within the photosynthetic membrane. Information on this concept

began with Robert Emerson's observation that absorbed far red light (>700 nm) produces a poor yield of photosynthesis but is strongly enhanced to high efficiency when shorter wavelength light (<700 nm) is supplemented (Emerson et al. 1957).

This observation might indicate that photosynthesis requires the excitation of two different pigments or antennae systems. This corresponds also to the behavior of fluorescence light changes (Govindjee et al. 1960; Kautsky et al. 1960). In 1960 Hill and Bendall hypothesized that in photosynthesis two different photoactive components might be coupled in series (Hill and Bendall 1960). Experimental proof for such an interaction of two photosystems was provided in 1961 in three laboratories which demonstrated independently by different optical absorption changes that an intermediate reaction component can be oxidized by far red light, that is, by a Photosystem I, and can be reversed to the reduced state only by shorter wavelength light <700 nm, that is, by a Photosystem II (Duysens et al. 1961; Kok and Hoch 1961; Witt et al. 1961a, b). The nature of the two photosystems, however, remained unknown at the time. But, in those years photosynthesis research made important steps ahead by optical inspection of fast intermediate reactions and their chemical components, as reviewed in those days by Kamen (1963) in his book 'Primary Processes of Photosynthesis.'

Components and spatial organization of the photosystems – analysis by repetitive light-pulse spectroscopy and a molecular voltmeter

Since the reactive components in photosynthesis are very short-lived and present in low concentrations, the absorption changes of the events are extremely small or even buried in noise. In 1932, Emerson and Arnold (1932) had introduced repetitive flash technique for measuring oxygen evolution that led to the concept of 'photosynthetic unit.' A major step ahead was realized in the 1960s with the introduction of the repetitive light-pulse spectroscopy (Witt 1967; Witt and Rüppel 1969). Periodic flash excitation and averaging of the optical signals in special devices increased the signal/noise ratio in n-flashes by a factor $\sqrt{n}$. In this way the ratio was increased up to 100-fold. Thereby also the time resolution of the events was extended from ms to μs and, in 1967, to the ns-range with the development and installation of the first Q-switched ruby laser adapted by the Ratheon Company for our demands for working repetitively at 5 cps. Later this range was extended beyond 1 ns with the availability of ps-lasers. With the repetitive technique different laboratories discovered new time-resolved spectra and reaction intermediates. In the Max-Volmer-Institute in Berlin, 10 transient optical difference spectra – especially those of the photosystems – were analyzed, and the constituents responsible, as well as their physical and chemical reaction sequences, were elucidated. [Chlorophyll *a* P700, Chlorophyll *a* P680, plastoquinone, Q_A, pool of plastoquinones, manganese, tyrosine, chlorophyll triplet, carotenoid triplet, localized and delocalized electrochromic changes, indicating different electric events (see below).] For an overview see Witt (1996a), for further historical details Witt (1991).

One outstanding light-induced optical difference spectrum – characterized by a typical asymmetrical shape observed at different wavelengths in the spectrum – could not be attributed to the normal type of reactions. Help in finding the reason for this spectrum was the observation made in 1966 that phosphorylation as well as the spectrum in question are selectively inhibited by an uncoupler but with little influence on electron transfer reactions (Rumberg et al. 1966; Witt et al. 1966, both reviewed in Witt 1971). Considering that in those years it was hypothesized that ATP formation is driven by a transmembrane electrochemical gradient of protons (Mitchell 1961), it became likely that the spectrum might reflect a transmembrane electric field or a proton gradient; the latter was unlikely because of the fast rise (<20 ns) of the spectrum. Clarification of this suggestion has been supported by essential contributions based on the work of Wolfgang Junge and of Roland Reich. It was found that addition of ionophores increasing the membrane permeability accelerates the decay of the spectrum, giving evidence that these optical signals indicate changes of a transmembrane electric field (Junge and Witt 1968; Emrich et al. 1969). This conclusion became convincingly visible when the membrane pigments were arranged in an artificial multi-layer across which an external field was applied in the dark, since absorption changes were observed to correspond closely to the spectra of changes induced by light *in vivo* (Schmidt et al. 1971, 1972). The field-indicating absorption changes are caused by a shift of the absorption bands of membrane pigments, induced by the interaction of the created field with the electronic energy levels of the pigments. These 'electrochromic band shifts' can be used as a molecular multimeter, signaling voltages, currents, and formation of charges from the functional membrane, without time restriction; thereby also topologies of the constituents of the photosystems become visible

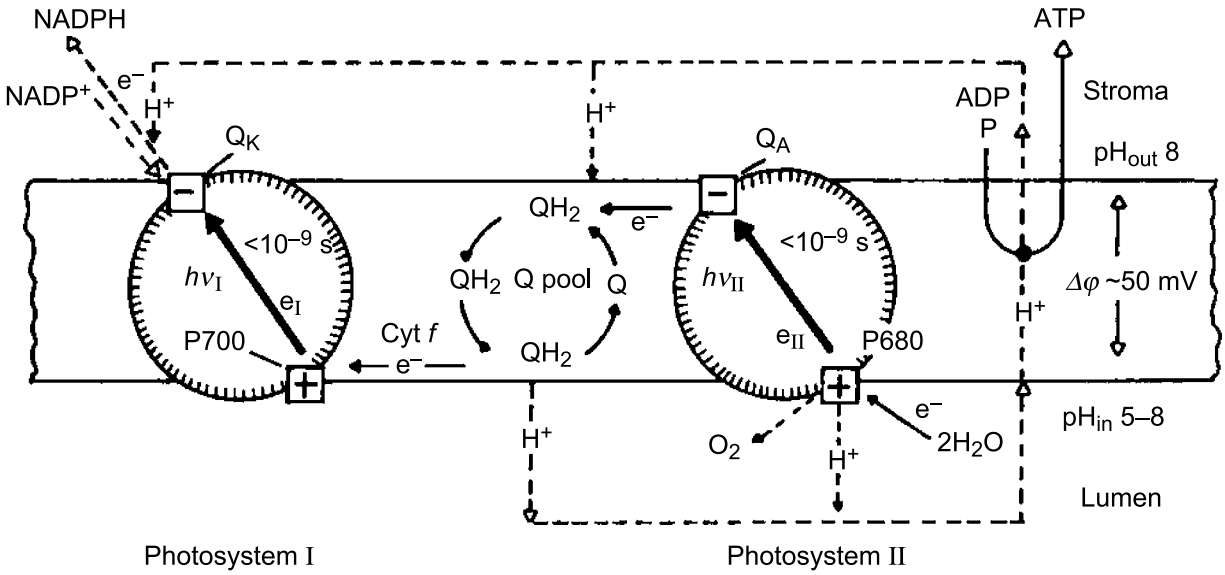

Figure 1. Simplified scheme of the primary reactions in photosynthesis elucidated in the 1960s. The pathways of the electrons and protons in the photosynthetic membrane and the subsequent reactions of water oxidation, $NADP^+$ reduction and ATP formation are driven by the cooperation of Photosystems I and II (Schliephake et al. 1968).

(Witt 1971, 1979). In this way, unique functional and structural qualities of the photosystems have been elucidated [for an overview, see Ke (2001)]. This paper reports on the architecture of PS I and PS II.

Two transmembrane charge separation events and their identification as primary act of light energy conversion – organization of the electron donors and acceptors

Up to the 1960s it was not considered that the light-induced *primary* electron transfer in photosynthesis might occur perpendicular to the membrane plane. However, it became spectroscopically evident that besides the coupling of two light reaction centers a further unique feature of the primary events is the vectorial transfer of electrons from excited primary donors across the photosynthetic membrane to electron-stabilizing acceptors on the opposite side. This charge separation was observed by the formation of the accompanying transmembrane *electric field* indicated by the electrochromic absorption band shifts discussed in the previous section. This event was characterized by the following properties.

(1) The *rise time* of the electric field (Wolff et al. 1969) corresponded to that of the photooxidation of the primary electron donor P700 in PS I (Witt and Wolff 1970), in those days <20 ns. This coincidence – later also measured at greater time resolution – identified this charge separation as a *primary act*.

(2) When one photosystem was blocked, the field *amplitude* was halved indicating a transmembrane charge separation in PS I as well as in PS II (Schliephake et al. 1968).

(3) The evaluated *polarity* of the field (positive inside) gave structural evidence that the primary electron donors (P700 and P680, see below) are located at the *lumenal* side of the membrane, and the stabilizing electron acceptors (quinones) at its *stromal* side (for details, see Witt 1971, 1979).

Thus the absorbed light energy is converted to the energy of a transmembrane charge-separated state. This state is built up by a reducing and oxidizing species on either side of the membrane. This localized dipole field first generated in the reaction center is subsequently delocalized within μs over the entire membrane. The energy of this *charged membrane battery* is used for water oxidation, $NADP^+$ reduction, and phosphorylation of ADP to ATP (see Figure 1). These products are used for reduction of CO_2 to energy-rich biochemical compounds (see Benson 2002; Jagendorf 2002; Bassham 2003, these historical issues).

The primary electron donor chlorophyll P700 of PS I – indication of a dimeric state

A pigment, P700, with light-induced absorption change at 700 nm was discovered by Kok (1956). Changes observed later at 438 nm (Kok 1961; Witt et al. 1961b) indicated that P700 is a special chloro-

phyll *a* of PS I which is oxidized by light. The difference spectrum of the photooxidation, $P700^{+\bullet}$–P700, inducible also at cryogenic temperatures of ∼125 K (Witt et al. 1961b), identified P700 as primary electron donor of PS I, that is – according to the previous section – P700 is located at the lumenal membrane side. The rise time was <20 ns (Witt and Wolff 1970). The nature of its primary stable electron acceptor, a phylloquinone Q_K (see the section 'The membrane spanning chlorophyll–quinone couple...'), was at that time not identified. The excited P700 is a strong reductant which, via different electron carriers, finally reduces $NADP^+$ (see later). The spectrum of P700 oxidation was extended by Rumberg and Witt (1964) and the qualities of P700 characterized by Rumberg (1964). Later on, in isolated and enriched PS I a double band in the red region at 682 and 700 nm was observed; this shape was explained by an excitonic coupling of two pigments and it was concluded that the primary electron donor P700 might be a chlorophyll dimer (Döring et al. 1968a). A dimeric structure was also suggested later from EPR studies and named 'special pair' (Norris et al. 1971). The idea of a dimeric donor became important because it called for proof whether such a structure is characteristic also for primary donors of other RCs in photosynthesis. And, indeed, this became successively evident in the following years for different photosystems (see below). With respect to PS I, 25 years later, direct evidence for the proposal of a P700 dimer became available by X-ray structure analysis of PS I 3-D crystals (Witt et al. 1992; Krauß et al. 1993; Käß et al. 2001) (see below). The refined PS I structure at 2.5 Å resolution even shows that one of the two Chls is a $C13^2$ epimer of Chl *a* (Jordan et al. 2001), that is, P700 is a heterodimer. The observed epimer was in agreement with a biochemical analysis outlined 16 years earlier (Watanabe et al. 1985).

The primary electron donor chlorophyll P680 of PS II and its stable electron acceptor plastoquinone Q_A – a membrane spanning redox couple as reaction center

Based on a flash-induced spectrum with changes at 435 and 682 nm, a special chlorophyll *a*, named Chl-*a*-II, later denoted P680, was characterized as the primary electron donor in PS II (Döring et al. 1968b, 1969). The absorption change of P680 in the red region of the spectrum had been identified 1 year before (Döring et al. 1967). In contrast to P700, the difference spectrum of the photooxidation $P680^{+\bullet}$–P680 can be induced only by light below 700 nm indicating that it is the primary donor of PS II (see the first section). P680 is a Chl *a* with outstanding features. Its cationic radical $P680^{+\bullet}$ has one of the highest redox potentials found in nature (≥1.1 V; see below), and is thereby capable of water oxidation in the catalytic center of PS II. The discovery of P680 was much more difficult than that of P700, because the absorption changes of P680 overlap with the extremely intense Chl *a* fluorescence at ∼680 nm induced by the exciting flash light. Furthermore, the life time of $P680^{+\bullet}$ is, depending on the conditions, more than 100 times shorter than that of $P700^{+\bullet}$, and thereby masked by a 10 times greater noise level. These problems have been overcome by the repetitive light pulse technique (see the section 'Components, special qualities, and spatial organization of the photosystems...'). The strong fluorescence was eliminated by high frequency modulation of the measuring light combined with an amplifier tuned to the modulating frequency (Buchwald and Rüppel 1968; Döring et al. 1968b).

A plastoquinone molecule, Q_A (formerly named X-320), was identified, from single turnover flashes, with a spectrum with maximal changes in the UV at 270 and 320 nm (Stiehl and Witt 1968). (In 1963, L.N.M. Duysens and H.E. Sweers had postulated a chemically unknown quencher 'Q' of fluorescence as an acceptor of PS II). The spectrum of Q_A resembles that appearing when plastosemiquinone is produced *in vitro*. This assignment was also concluded from the kinetic behavior: the decay time of the difference spectrum in question, $Q_A^{-\bullet}$–Q_A, coincides with the rise time of the spectrum of a plastohydroquinone (Stiehl and Witt 1969) (see below), showing to be its precursor, that is, a plastosemiquinone. Later, the spectrum of Q_A was refined (van Gorkom 1974) and definitely determined in Gerken et al. (1989). The tightly bound Q_A can be reduced only to a semiquinone. The kinetics of Q_A reduction indicate that Q_A is the stable primary electron-trapping acceptor of P680, that is, located at the stromal membrane side and P680 at the luminal side (see the section 'Two transmembrane charge separation events...'). Thus, the reaction center (RC) of PS II became evident as a transmembrane-spanning redox couple P680–Q_A, functioning in a light-induced transmembrane charge separation P680–Q_A → $P680^{+\bullet}$–$Q_A^{-\bullet}$. The univalent cationic radical $P680^{+\bullet}$ extracts stepwise four electrons from the water-oxidizing tetranuclear Mn cluster within four light-induced turnovers. After these four turns one O_2 is released from two H_2O indicating that the cluster passes through four increased oxidized

states S_0–S_4 (Joliot and Kok 1975), see also Renger (2003). $Q_A^{-\bullet}$ reduces molecules of a plastoquinone pool (see below).

A plastoquinone pool – the pathway for electrons between PS II and PS I and for protons between the outer and inner aqueous phases

The spectrum assigned to plastohydroquinone (see above) appeared in longer flashes or in a train of single turnovers. The spectrum corresponds to that appearing when plastoquinone A is reduced *in vitro* in methanol (Stiehl and Witt 1968). The optical change *in vivo* disappears after extraction of the quinone but reappears after recondensation of synthetic plastoquinone. The maximal absorption changes *in vivo* indicate that a pool with a capacity of 5–10 Q molecules is located between PS I and PS II in the lipid bilayer of the membrane. The stepwise reduction of the Q pool by PS II via Q_A^- as intermediate causes proton uptake at the stromal side of the membrane and formation of QH_2. QH_2 diffuses within the membrane until it reaches a binding site at the lumenal side, where it is finally reoxidized and deprotonated by the oxidized P700 of PS I, in cooperation with a Cyt b_6f complex (see below). A stoichiometric coupling of 1:1:1 between stromal H^+ uptake, transmembrane electron transfer and lumenal H^+ release was measured in the absence of a so-called 'Q cycle' (Tiemann et al. 1979). In this way it became visible that the plastoquinone pool acts structurally as a transmembrane bridge for electron transfer between PS II and PS I that is coupled with proton translocation between the outer and inner aqueous membrane phases.

With respect to details of the reduction of the pool it was shown that, after two PS II turnovers, Q_A^- reduces a mobile Q of the pool twice. These reductions occur after Q has docked to a binding site B on protein subunit D1, where it is then named 'Q_B.' A special Q_B molecule does not exist. After uptake of two protons by $Q_B^=$, its fully reduced form is released into the pool and replaced by a new, oxidized Q from the pool, allowing a subsequent cycle of reduction and release (Bouges-Bocquet 1973; Velthuys and Amesz 1974) [see Vermeglio (2002) for a perspective on Q_B in purple bacteria]. With reference to details of the oxidation of QH_2, the catalytic function of the membrane protein Cyt b_6f, located between PS I and PS II, later became evident. The Cyt b_6f complex channels one electron of QH_2,via 2Fe–2S, Cyt f and a soluble electron carrier Cyt c_6 (or plastocyanin), towards the oxidized P700, and the second electron, via the Cyt b_6, back to a Q of the pool for a subsequent reduction. This so-called 'Q cycle' is described by Hauska et al. (1996); see also Hauska, this issue, and Crofts, this issue.

The membrane-spanning chlorophyll–quinone couple of PS II as reaction center model for other, different photosystems

Regarding the features of Photosystem II evaluated in the section 'The primary electron donor chlorophyll P680 of PS II...', by the late 1960s these had already given the first information on the construction of a photosynthetic reaction center in form of a membrane-spanning chlorophyll–plastoquinone couple functioning in a light-induced transmembrane charge separation. Years later, these characteristics of PS II were shown to be valid also for RCs of anoxygenic bacteria. In the purple bacterium *Rb. sphaeroides* a ubiquinone, Q_U, acts as a stabilizing electron acceptor of the primary donor P870 (Clayton and Straley 1970; Slooten 1972) and a transmembrane electric field generation, indicated by an electrochromic band shift, was also observed (Jackson and Crofts 1969) (see also Clayton 2002). In the RC of PS I a phylloquinone, Q_K, was identified as a stable electron acceptor of the primary donor P700 (Brettel et al. 1986; Malkin 1986) with a transmembrane charge separation measured between them (Schliephake et al. 1968) (see the section 'Two transmembrane charge separation events...'). In green filamentous bacteria a menaquinone, Q_M, was discovered as electron acceptor of the donor P885 (Vasmel and Amesz 1983). It remained to be clarified whether a napthoquinone, Q_N, acts as electron acceptor of the donor P840 in green sulfur and heliobacteria.

In subsequent years it was shown that between the chlorophyll and the quinone of the couple, two chlorins function as transient intermediate electron carriers. In PS II these chorins are a Chl *a* (see the section '3-D crystallization of PS II...') and a Pheo (Klimov and Krasnovskii 1981; Klimov 2003); in PS I they are two Chl *a* (see the section '3-D crystallization of PS I...'); and in purple bacteria they are a BChl (Deisenhofer et al. 1985) and BPheo (Shuvalov and Klimov 1976) (see also Parson 2003). The presence of these two chlorins is of importance because electron transfer from the excited primary chlorophyll donor P^*_{700} and P^*_{680} towards the quinones must be fast compared to the deactivation of the excited state into the

ground state. This requires a rapid removal of the electron, which is possible within ps along the π-electron system of the two neighboring chlorins, acting as a molecular wire, and with electron tunneling between them.

It has been generally outlined that RCs in photosynthesis belong to two different types, characterized by their electron acceptors: the quinone type (green bacteria, purple bacteria, and PS II) and the Fe/S type (green sulfur bacteria, heliobacteria, and PS I). However, the basic event common to both types of reaction center is the stabilization of the electrons transferred out of the primary electron donors across the membrane by trapping these through the quinones. In PS I, PS II and purple bacteria it was shown that all subsequent electron transfer steps from these reduced quinones take place after times which are at least two orders of magnitude greater than the times establishing these states.

In subsequent years, the transmembrane-oriented chlorine–quinone couple took shape through further structural and functional details elucidated in different laboratories. These details resulted in extended RC models of PS II, purple bacteria and PS I. Then, in 1985, a breakthrough came with the first X-ray structure determination of single crystals of the purple bacterial RCs presented by Hartmut Michel, Johann Deisenhofer and Robert Huber. With their model at 2.9 Å resolution, amazing principal news became visible (Deisenhofer et al. 1985; also see Allen, this issue). But their structure also amply confirmed the earlier features of the RC of PS II and purple bacteria as a membrane-spanning chlorophyll–quinone model identified by the above discussed spectroscopic methods before X-ray structural results came along. An unexpected discovery was that *two* such symmetrical chlorine–quinone branches are present per RC. But the second branch was shown to be inactive in electron transport. How this unidirectionality of electron transfer is regulated is not yet clearly understood. Later, two branches were also discovered in PS I and PS II (see the sections '3-D crystallization of PS I. . .' and '3-D crystallization of PS II. . .').

Revealing structural news by getting to the roots through change from plant material to cyanobacteria

Following the description of the basic RC structure of the photosystems first based on spectroscopic analysis, an essential second step towards an improved structural analysis of Photosystems I and II was realized in the 1980s by changing the starting material from plants to cyanobacteria. The latter are the only bacteria capable of water oxidation and possibly also the most ancient species capable of water cleavage. Thermophilic bacteria grow in hot springs. They are of simpler construction [no PS I peripheral antennae, that is, a light harvesting complex (LHC) is absent], of more robustness, and are easier to isolate and purify. Grown in large reactors, high yields of protein are available, allowing extensive screening for optimization of the isolation, purification and crystallization of the photosystems (Schatz and Witt 1984a, b; Rögner et al. 1987; Dekker et al. 1988). Based on these improvements, highly purified reaction centers of PS I and PS II isolated from the thermophilic cyanobacterial material of *Synechococcus elongatus* became the essential prerequisite for revealing the structural organization of the two systems. In this context the work of Günther Schatz, Matthias Rögner, Jan Dekker and Egbert Boekema as well as the brilliant technical assistance of Ms Dörte DiFiore was of great significance for the progress in this field in the following years.

Size and shape of the supra-molecular complexes of the photosystems – first evidence for a PS I trimer and PS II dimer

The first information on the supramolecular structure of the photosystems was obtained by electron microscopy at ~20 Å resolution with highly purified PS I and PS II core complexes from *S. elongatus*. Structures were visualized by averaging the aligned images of single complexes with a digitizing camera. Photosystem I complexes showed a trimeric organization, each trimer having a diameter of 190 Å and a width of 60 Å (Boekema et al. 1987). The structure resembles a clover leaf (see Figure 2A). Each monomeric subunit within the trimer represents a functional PS I unit (Rögner et al. 1990). The trimer was subsequently confirmed (Ford and Holzenburg 1988). PS II, in contrast, shows a monomeric and dimeric structure, the latter with dimensions of 155–185 Å × 120–150 Å × 58–65 Å (Rögner et al. 1987; Dekker et al. 1988) (see Figure 2B). It is very likely that the trimer of PS I and the dimer of PS II are the active forms *in vivo* (Hladik and Sofrova 1991). Years later this 'electron microscope image analysis' of single particles of photosynthetic material was applied to different supercomplexes of PS II, providing

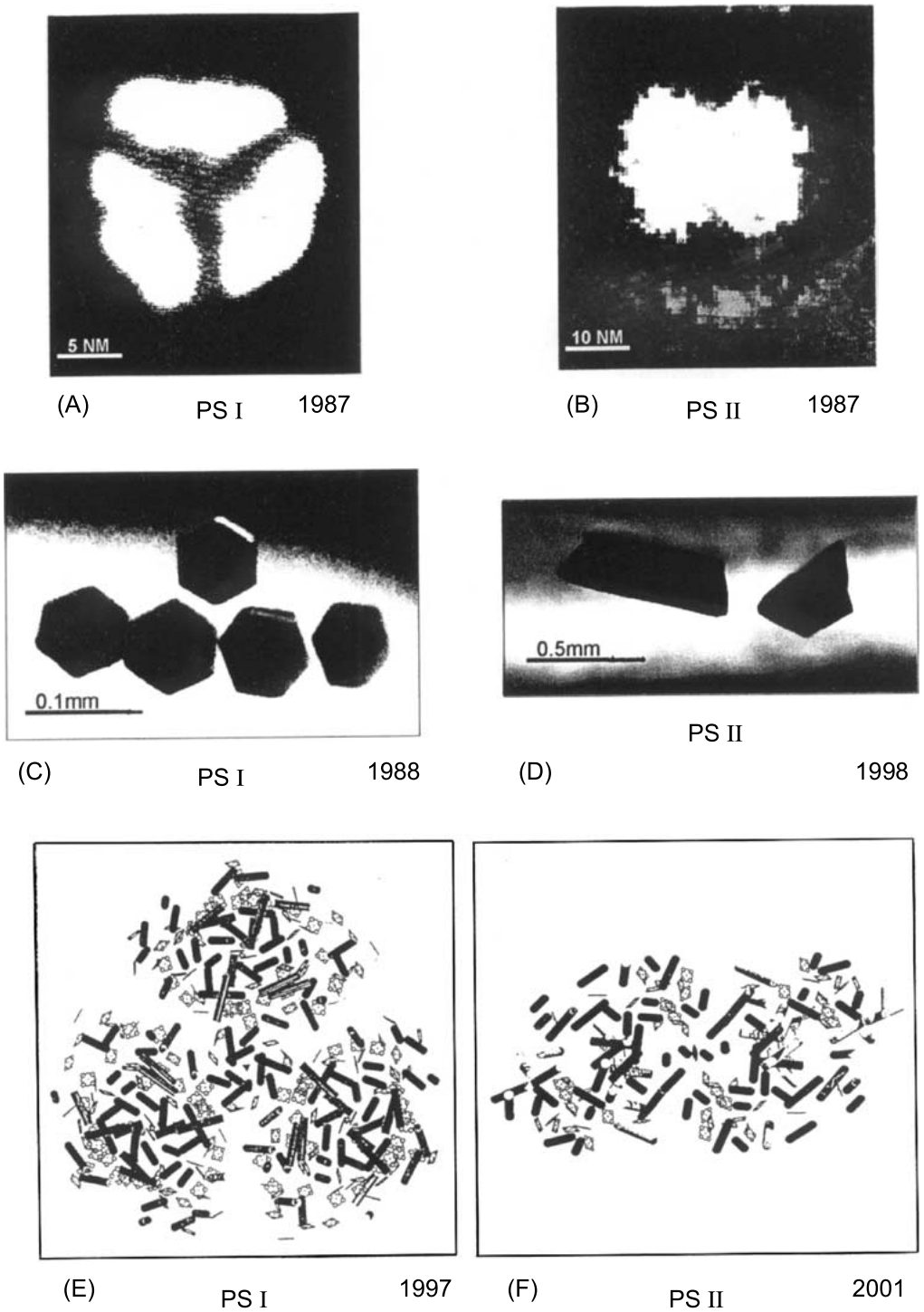

Figure 2. (A) Isolated PS I trimer; (B) PS II dimer from cyanobacteria *Synechococcus elongatus* pictured by electron microscopic image analysis (see the section 'Size and shape of the supra-molecular complexes of the photosystems . . .'); (C) Crystals of the PS I trimer (see the section '3-D crystallization of PS I . . .'); (D) Crystals of the PS II dimer (see the section '3-D crystallization of PS II . . .'); (E) X-ray structure analysis of PS I trimer at 4 Å resolution (see the section '3-D crystallization of PS I . . .'); (F) X-ray structure analysis of PS II dimer at 3.8 Å resolution (see the section '3-D crystallization of PS II . . .'). (E) and (F) indicate the organization of the Chls and helices with view onto the membrane plane.

details on their organization (Kuhl et al. 1999; Nield et al. 2000; also see Barber, this issue).

In a third step towards structural details of PS I and PS II, the isolated trimers and dimers were used to explore the conditions of 3-D crystallizations of cyanobacterial material. This work was encouraged by the successful X-ray structure analysis of the RC from purple bacteria (Deisenhofer et al. 1985), although we were aware that PS I and PS II are much more complex, with many more subunits in PS I and PS II and more than a hundred cofactors in PS I. We started with PS I trimers, because the yield of this isolated complex was at that time much higher than that of the PS II dimer. First PS I crystals were obtained in 1987 (Ford et al. 1987; Witt et al. 1987). Crystals suitable for structural analysis were successfully produced one year later (see below).

3-D crystallization of PS I – X-ray structural analysis successively established from 6 to 2.5 Å resolution

According to biochemical analysis, the PS I monomer of *S. elongatus* contains 11 subunits (Golbeck 1994). The PS I trimer – a large membrane protein with a mass of more than 1000 kDa (see below) – was solubilized in the detergent β-D-maltoside and crystallized with the batch method in capillaries at pH 7, 4–8 °C, and 1–5 mM Chl on the 'salting out' branch of the solubility curve of proteins, whereby polyethylene glycol at concentrations up to 6% w/w was used as the precipitating agent. In contrast to our earlier results in 1987, the protein concentration used was up to 100 times higher. Needle-shaped crystals were obtained of length up to 1 mm with hexagonal cross-section (see Figure 2C), and these diffracted X-rays up to 4 Å (Witt et al. 1988). It is the largest and most complex membrane protein which has been crystallized as yet. At the same time also the 'salting in' branch of the solubility curve of proteins was inspected as to its suitability for crystallization. We obtained crystals by working without any crystallization mediators: the salt concentration of the protein solution was simply diluted thereby running the 'salting in' procedure of proteins in reverse, that is, water was used as precipitating agent. Unexpectedly large numbers of small crystals ($\leq$0.1 mm) appeared in minutes. These were used for a further purification. After resolubilization of the crystals by addition of salt and by subsequently repeated dilution of the salt with water, but outlined slowly by programmed dialysis against low salt concentration and ion strength respectively, large and strongly improved mm-crystals with lower mosaic spread were obtained within 1–2 days. The growth was also initiated with the small crystals as seed material. This 'reverse of salting in crystallization' was the basis for all structural determinations of the PS I structure from 6 Å up to 2.5 Å resolution. This method, described in Witt et al. (1992) and Witt (1996b), has been developed since 1987 by the author together with his wife, Ingrid Witt. Her creative engagement has been indispensable for the results described here. Subsequently, Petra Fromme joined the project and continued the crystallization with important contributions for the determination of the high resolution structure of PS I (see below).

The space group of the crystallized PS I trimer is hexagonal, $P6_3$, with unit cell constants a = b = 286 Å, c = 167 Å, and two trimers per unit cell. The relatively large unit cell and mosaicity of the crystal induces close spacing and diffuse reflections in the X-ray diffraction images. Thus, the availability of the small beam divergence and high intensity of the X-rays from synchrotron sources became important. The crystals are stable in concentrated sucrose solution, which was used as cryoprotectant for improved X-ray diffraction measurements at 100 K. Phase determination was carried out by multiple isomorphous replacement using heavy-atom derivatives.

As a basis for the structural interpretation of the calculated electron density maps, the genes encoding the 11 subunits of the PS I monomer were isolated and the sequence of amino acid residues in the subunits deduced (Mühlenhoff et al. 1993), indicating together with the content of the cofactors (see below) a total mass of ca. 1020 kDa for the PS I trimer. A first structural model of PS I was proposed at 6 Å resolution (Witt et al. 1992; Krauß et al. 1993). The structure indicated *inter alia* 48 cofactors and two electron transfer branches with two chlorophylls for P700. Through a more improved electron density map a structure at 4 Å resolution became available (Krauß et al. 1996), followed by a comprehensive, structural model at this resolution (Schubert et al. 1997) (see Figure 2E). Through the subsequent systematic application of the micro- and macro-seeding technique and purification to perfection (α-isomer of detergent <0.1% and monomer of PS I <0.01%, both of the total), Petra Fromme improved and extended ingeniously the crystal quality to 3.3 Å resolution (Fromme and Witt 1998) and, recently, even to 2.5 Å (Jordan et al. 2001). The electron density map at 2.5 Å resolution provides a highly refined structure of the RC core

complex and antenna system of PS I in atomic detail. (Also see Fromme and Mathis, this issue; Nelson and Ben-Shem 2002.)

Per PS I monomer 127 cofactors (∼30% of the mass of PS I) were identified: 96 chlorophylls, 22 carotenoids, 2 phylloquinones, three 4Fe–4S clusters, 4 lipids, and 201 water molecules. To the 11 subunits of PS I, 31 transmembrane α helices have been assigned. Additionally, a 12th subunit containing only a single α-helix was observed. The structure shows how these components are spatially organized within the scaffolding built by the helices, as well as within the three extrinsic subunits on the stromal side (see Figures 3A–C). The results provided information on the interaction between the cofactors and their immediate environment, information that is indispensable for understanding their function. This model is characterized by many exceptional features (see e.g. Jordan et al. 2001). A few characteristics are briefly described below.

The *electron transfer* chain ETC of a PS I monomer contains in the main subunits PsaA and PsaB two rather symmetrically arranged branches α and β of cofactors for electron transfer similar to those first observed in purple bacteria in subunits D1 and D2 (see the section 'The membrane-spanning chlorophyll–quinone couple...'). In PS I, five C-terminal transmembrane helices each of PsaA and PsaB coordinate the cofactors resulting in three consecutively arranged Chl pairs and a phylloquinone, Q_K, pair. These cofactors span the membrane ending in one 4Fe–4S cluster, F_X, located at the pseudo-2-fold axis relating PsaA to PsaB (Figure 3B). From there two 4Fe–4S clusters, F_A and F_B, arranged in series and coordinated to the extrinsic subunit PsaC, provide a bridge to the soluble electron acceptor ferredoxin Fd. Fd reduces $NADP^+$ via a reductase (see Shin, this issue). The first Chl pair (yellow) of the ETC is assigned to the primary donor P700. In contrast to PS II and the reaction center of purple bacteria, it is seen, in PS I, that the primary donor is a heterodimer in which that Chl of P700 bound to the α-branch is three times hydrogen-bonded and, in addition, is an epimer of the other Chl (see the section 'The primary electron donor chlorophyll P700 of PS I...'). The hydrogen bonding of the Chl increases its oxidation potential suggesting that only the β-branch is active in electron transfer. Histidine residues of the nearby helices act as polarizable axial ligands to the Mg^{2+} ions of these two Chls of P700. The Mg^{2+} ions of the second Chl pair, however, are each ligated by a water molecule which is hydrogen-bonded to amino acid residues; this second pair is new and has not been spectroscopically identified before. Unusual is that the hard acid Mg^{2+} ions of the third Chl pair are ligated by the soft base sulfur atoms of methionine residues. The ETC and antenna system are well separated from each other (see below). However, one antenna Chl each is located between the third Chl pair of the ETC and the antenna system, shortening the distance between both suggesting that these Chls function as a bridge for the excitons from the antenna system to the ETC. This may imply an exotic transfer route for the *exciton* energy in direction from the antenna system via the third and second Chls to P700 and consequently followed by an *electron* transfer from the excited P700 along the same route but in the opposite direction and from the third pair further on to the phylloquinones, Q_K. Whether one or two branches are active in electron transfer is still a matter of debate (Jordan et al. 2001). Kinetic investigations indicate that both branches are used, but that their electron transfers have different rate constants (Joliot and Joliot 1999).

With respect to the *antenna system* of a PS I monomer 79 Chls are bound to the large subunits PsaA and PsaB; only 11 of the 90 antenna Chls are coordinated by smaller subunits at the outer side. In PsaA and PsaB 43 Chls fill the central antenna domain. These Chls are arranged in the shape of an elliptical cylinder with a wall across the entire membrane depth. The two peripheral antenna domains contain 18 Chls each. They are arranged in two layers towards the stromal and lumenal side (see Figure 3C). The six N-terminal transmembrane helices each of PsaA and PsaB are engaged in the coordination of these peripheral Chls. The helices are arranged as trimers of dimers. The wall of the central domain is separated from the ETC by distances of 20–40 Å. Even P700 is ∼20 Å from the antenna Chl, a distance sufficient to prevent electron transfer and reduction of the antenna Chls by the excited P700. On the other hand, to support excitation of P700 despite this large 20 Å gap between the antenna and P700, it is possible that the above-discussed exotic exciton pathway, via the two bridging Chls towards P700, might be used preferentially. The antenna system of PS I is unique in that it is fused with those parts of the subunits PsaA and PsaB in which the ETC is suspended (see above). This is different from PS II and purple bacteria which are equipped with antenna systems located in subunits separated from those containing the ETC (see the section '3-D crystallization of PS II...').

The outstanding completeness of the PS I model becomes visible not only with the location of

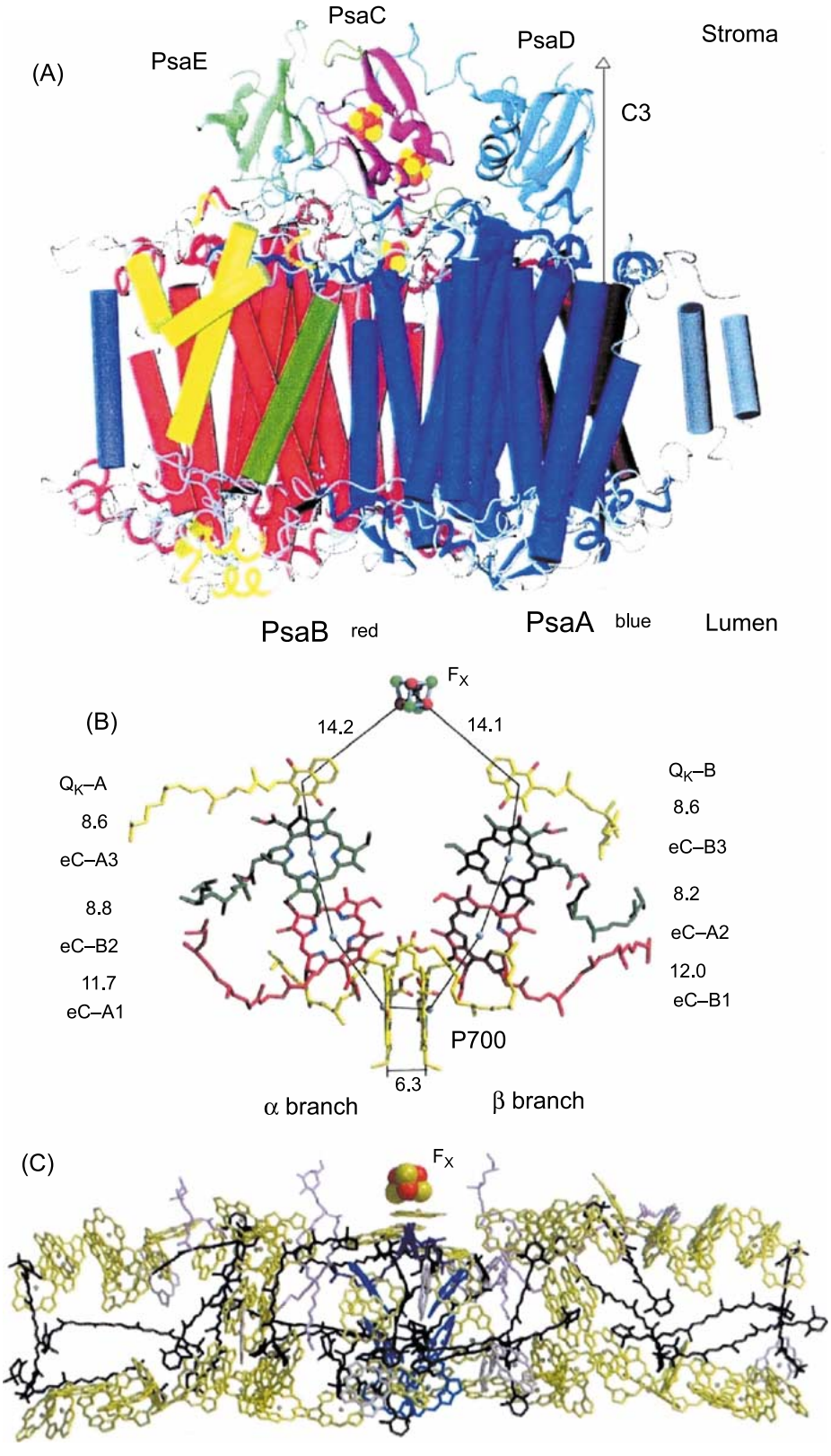
(A)
PsaC
PsaE
PsaD
Stroma
C3
PsaB red
PsaA blue
Lumen
(B)
F_X
14.2
14.1
Q_K–A
8.6
eC–A3
8.8
eC–B2
11.7
eC–A1
Q_K–B
8.6
eC–B3
8.2
eC–A2
12.0
eC–B1
P700
6.3
α branch
β branch
(C)
F_X

96 antenna- and cofactor-Chls but also with the estimation of their orientation in space as well as within the planes of their headgroups. All chemically identified 22 carotenoids, deeply inserted into the membrane, have been located; in addition, their directions and immediate van der Waal contacts ($\leq$3.6 Å) with 60 Chls have been elucidated. Besides the light harvesting function of the carotenoids in the blue range, their 60 contacts with the Chls are a prerequisite for facilitating photoprotection by quenching, via a Dexter charge transfer mechanism, excited Chl triplet states, ^{3}Chl*, created when the photochemical trap is closed at excessive light intensities. Through this reaction, $^3\text{Chl}^* + {}^1\text{Car} \rightarrow {}^1\text{Chl} + {}^3\text{Car}^*$, formation of toxic singlet oxygen $^1O_2^*$ is prevented, which otherwise would be created by the reaction of $^3\text{Chl}^* + {}^3O_2 \rightarrow {}^1\text{Chl} + {}^1O_2^*$ (Wolff and Witt 1969).

The PS I model allows an extensive comparison between oxygenic and anoxygenic photosynthetic systems and conclusions on their common ancestor. In this context it was also possible to propose – based on the structure of PS I and purple bacteria – the scaffolding of all helices of the core complex of PS II as well as of the helio- and green-sulfur bacteria (Schubert et al. 1998).

With the availability of the PS I crystals new directional structural information has been obtained also with EPR and ENDOR techniques by measurements on single crystals in dependence on their orientation. This was performed on charge separated states of the RC of PS I and recently also of PS II. (For details see Bittl et al. 1997; Kamlowski et al. 1998; Zech et al. 2000; Hofbauer et al. 2001; Käß et al. 2001; Lubitz 2002.)

Modeling and electron- and X-ray crystallography of PS II

Before suitable PS II 3-D crystals became available, information on the possible PS II structure was gained – besides electron-microscopy (see the section 'Size and shape of the supra-molecular complexes of the photosystems. . .') – by computer modeling of the core of the RC of PS II (Ruffle et al. 1992; Vermaas et al. 1993; Svensson et al. 1996; Xiong et al. 1996), based on the homology between the L/M subunit of purple bacteria and the D_1/D_2 unit of PS II (Trebst 1985; Michel and Deisenhofer 1988). Vermaas et al. (1993) assigned amino acid residues as possible ligands for manganese based on mutagenesis studies. Xiong et al. (1996) presented a model including the RC cofactors. Svensson et al. (1996) predicted a larger distance between the two chlorins in P680, that is, that P680 may not be a special pair.

Electron crystallography was applied to 2-D crystals prepared from PS II (Rhee et al. 1997, 1998; Hankamer et al. 1999). This method is principally restricted to lower resolution levels compared to X-ray crystallography. For a PS II fragment D1-D2-CP47 without water-oxidizing activity Rhee et al. obtained a resolution of 8 Å (for a review, see Rhee 2001). This work reveals the organization of 16 helices as well as the likely positions of 6 tetrapyrrole cofactors showing that they are similarly organized as those in corresponding fields of the RC from purple bacteria and PS I, ~14 chlorophylls were assigned to the CP 47 subunit. The organization of the helices confirmed the arrangement proposed for PS II, referred to in the first full paragraph in the left-hand column (Schubert et al. 1998). The work was extended by Hankamer et al. (2001) to the CP43 unit and the material of higher plants.

Reports on the 3-D crystallization of the RC of PS II were published from 1998 on (Adir 1998; Zouni et al. 1998; Kuhl et al. 2000; Shen and Kamiya 2000). The first structural results by X-ray crystallography of 3-D crystals of PS II were obtained in 2001 (see below).

3-D crystallization of PS II – first crystals capable of water oxidation – X-ray structure analysis at 3.8–3.6 Å resolution

Fully active PS II dimers from the cyanobacterium *S. elongatus* were isolated and prepared without the phycobilisome antenna (Rögner et al. 1987; Dekker et al. 1988). The PS II monomer is composed of at least 17 subunits (Barry et al. 1994). The homodimer has a mass of ~700 kDa. This was crystallized with polyethylene glycol as precipitating agent analogous to the conditions of the 'salting out' crystallization

Figure 3. (A) Side view of a monomer of the PS I trimer indicating the helices of the different subunits. View direction is along the membrane plane. The three membrane extrinsic subunits PsaE, PsaC, and PsaD are located on the top of the transmembrane helices. (B) Cofactors of the membrane intrinsic part of the electron transfer chain (ETC) from P700 up to the FeS-cluster, F_X. View along the membrane plane. The Chls are denoted eC, followed by A and B indicating the coordination of the cofactors with PsaA and PsaB, respectively. Note the crossover at the second pair. (C) Side view of that part of the membrane intrinsic antenna system which is coordinated with 79 chlorophylls and most of the 22 carotenoids to the subunits PsaA and PsaB. Eleven Chls are coordinated outside by smaller subunits (Jordan et al. 2001).

developed for PS I (see the section '3-D crystallization of PS I. . .'). Through comprehensive screening Athina Zouni has elucidated the conditions for the growing of PS II crystals suitable for structure analysis (see Figure 2D) (Zouni et al. 1998). The crystals with size up to 1 mm belong to the ortho-rhombic space group $P2_12_12_1$ with unit cell constants $a = 134$ Å, $b = 227$ Å, and $c = 310$ Å. The unit cell accommodates four dimers.

However, it was by no means self-evident that the sensitive water oxidizing complex of PS II was not changed into an inactive conformation through the crystallization procedure. Therefore, first the activity of the PS II crystals themselves was directly measured. In flash light excitation the crystals show highly active water oxidation measured by oxygen evolution and corresponding proton release (Zouni et al. 2000) yielding the expected stoichiometry of four H^+s per O_2. The crystals are very stable. After 10,000 flashes the activity only decreases by 30%, whereas with PS II in solution by 70%.

The X-ray diffraction of these crystals at 100 K, using glycerol as cryoprotectant and radiation from synchrotrons, resulted in electron density maps at 3.8 and 3.6 Å resolution (Zouni et al. 2001a, b). Phases were determined by multiple isomorphous replacement using heavy-atom derivatives. The successful structure analysis has been performed by Peter Ort and Norbert Krauß. In the current model, 44 cofactors have been identified per PS II monomer: 32 chlorophylls, 2 pheophytins, 1 plastoquinone, 2 heme irons, 1 non-heme iron, 2 tyrosine residues, and 4 manganese atoms. Thirty-six transmembrane α-helices have been localized per monomer (see Figure 2F). These belong to 14 subunits PsbA to PsbN and PsbX located in the membrane.

With respect to the spatial organization of the 36 helices, two groups of five transmembrane helices were assigned to the main subunits D1 (PsbA) and D2 (PsbB). These helices coordinate the cofactors of the ETC in two pseudo-symmetrical branches, similar to those helices in the L and M subunits of purple bacteria and the five innermost helices of the C-terminal domains of the PsaA and PsaB subunits of PS I (see above).

In the core *antenna system* of PS II, which is located in the separated subunits CP43 and CP47, six transmembrane helices each are arranged as trimers of dimers; the coordinated ∼26 Chls are arranged in two layers close to the lumenal and the stromal membrane side (see Figure 4, bottom). This arrangement resembles that of the peripheral antenna domain in Figure 3C of the subunits PsaA and PsaB in PS I coordinating 36 Chls (see the section '3-D crystallization of PS I. . .'). Of further helices two belong to the α and β subunits of Cyt *b*-559 and eight of the remaining 12 helices to the small subunit H to N and X with one helix each; four helices have not been assigned as yet.

It must be noted that PS I contains, in the PsaA and PsaB unit, besides the two peripheral antenna region with 36 Chls, a central domain surrounding the ETC with a wall of 43 Chls functioning as an efficient path for excitons between the peripheral antenna region and the ETC (see Figure 3C). However, the corresponding central domain 'surrounding' the ETC in PS II is occupied only by two Chls, Chl z_{D1} and Chl z_{D2} (see Figure 4, bottom). This raises the question whether this 'empty' field in PS II is a necessary consequence of the 'photo damage and repair process' in the D1 protein. The damage–repair cycle gives PS II the safety to overcome the threat of destruction by the high oxidation power of P680, producing toxic oxidative species in excessive light intensities. In the repair it is possible that a broken D1 unit is disassembled and a newly synthesized D1 is reassembled. [For a perspective on photoinhibition, see Adir et al. (2003).] The cycle is optimized when repair keeps up with damage. Perhaps the absence of the expected antenna Chls in the discussed domain is even advantageous for an optimal balance and maybe PS II is thereby optimized for *regulation of safety* rather than for efficiency. More information may become available when at higher structural resolution new cofactors for example, carotenoids become visible in this field and their function will be understood.

The *electron transfer chain* (ETC) starts with two Chl *a* molecules, P_{D1} and P_{D2}, at the lumenal side; they have been assigned to P680 of PS II (see Figure 4). Their head groups are parallel to each other and perpendicular to the plane of the membrane. Based on the homology between PS II and purple

Figure 4. Top: Arrangement of the cofactors of the electron transfer chain in subunit D1 and D2 of Photosystem II. View direction along the membrane plane. The center-to-center distances (Å) and the pseudo C2 axis relating D1 to D2 are indicated. *Center*: *Left*: (a) Mn cluster with view along the membrane plane; the long axis of the cluster points towards the lumen tilted ∼23° against the plane; (b) view onto the plane. *Right*: Cyt *b*-559 with view along the membrane plane (see the section '3-D Crystallization of PS II . . .'). *Bottom*: Special side view of the ETC and antenna system along the membrane plane.

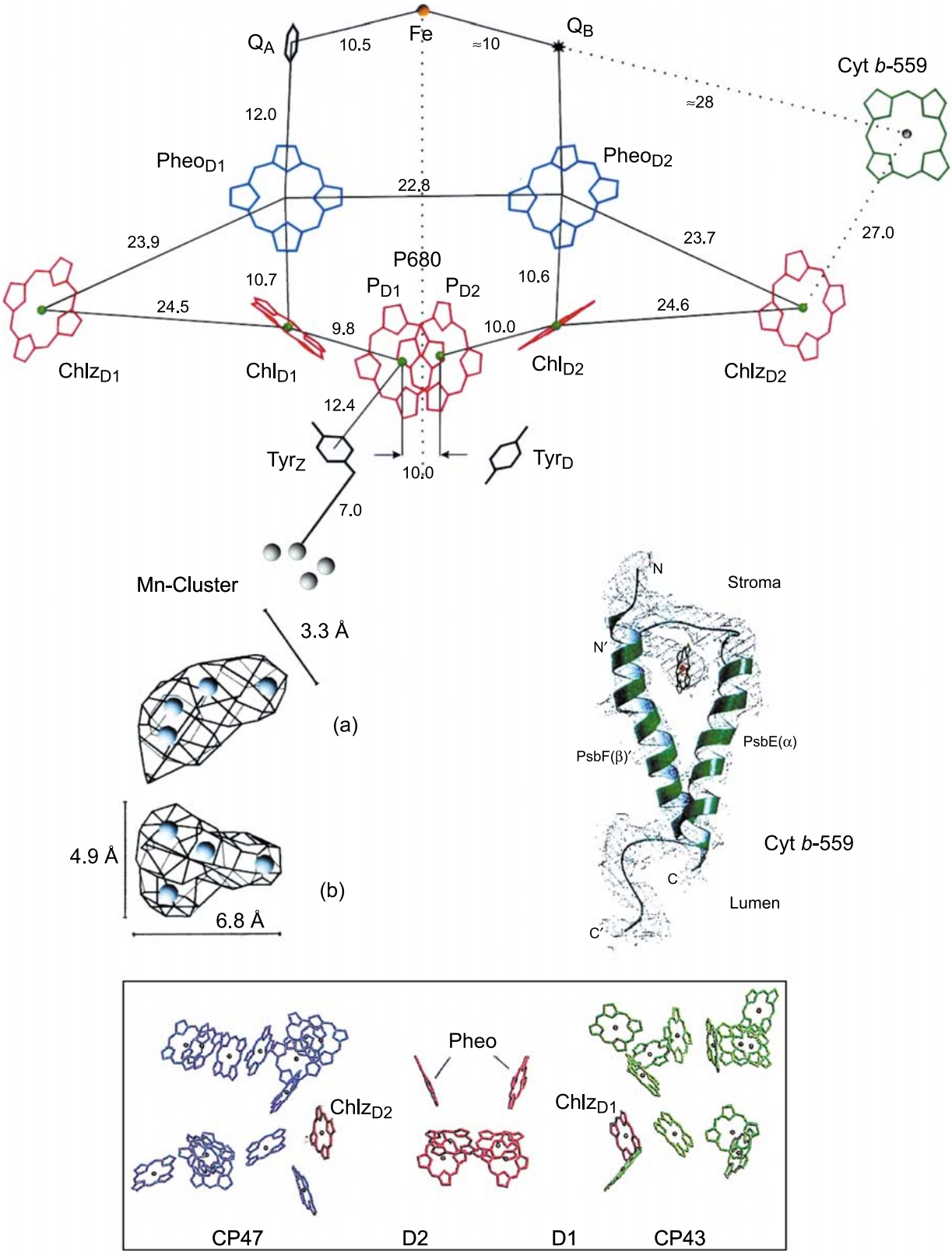
Q_A
Fe
Q_B
10.5
≈10
Cyt b-559
≈28
12.0
Pheo_D1
Pheo_D2
22.8
23.9
23.7
27.0
P680
P_D1
P_D2
10.7
10.6
24.5
24.6
9.8
10.0
Chlz_D1
Chl_D1
Chl_D2
Chlz_D2
12.4
Tyr_Z
Tyr_D
10.0
7.0
Mn-Cluster
3.3 Å
(a)
4.9 Å
(b)
6.8 Å
N
Stroma
N′
PsbE(α)
PsbF(β)′
Cyt b-559
C
Lumen
C′
Pheo
Chlz_D2
Chlz_D1
CP47
D2
D1
CP43

bacteria P_{D1} and P_{D2} are believed to be coordinated by D1-His 198 and D2-His 197. Towards the stromal side, P680 is followed by a pair of Chl_{D1} and Chl_{D2}, tilted by ∼30° against the membrane plane, corresponding to the 'accessory' BChls in purple bacteria. Further up a pair of pheophytins is located, $Pheo_{D1}$ and $Pheo_{D2}$ with their planes roughly perpendicular to the membrane plane. Two extra Chl $z_{D1,D2}$, not present in purple bacteria, are located at the periphery of the ETC ∼34 Å apart from the pseudo C2 axis running through the non-heme iron in the center of the core complex. The six chlorins in the RC of PS II correspond to the number determined biochemically by Eijekelhoff and Dekker (1995). The terminal electron acceptor of P680, the tightly bound plastoquinone Q_A is located on the stromal side of subunit D2. The putative docking site of the mobile Q_B (see the section 'A plastoquinone pool. . .') at a corresponding symmetrical position of subunit D1 was not occupied. The symmetry of the ETC is broken by the presence of one Cyt *b*-559 identified with its heme iron located near the stromal side at the periphery of D2, and by the location of the Mn cluster on the lumenal side close to the surface helix CD and the C-terminus of D1. Located between P680 and the Mn cluster in D1 is the tyrosine Tyr_Z; its counterpart in D2, Tyr_D, not essential for water oxidation, is placed symmetrically to Tyr_Z. When P680 is oxidized its unpaired electron $P680^{+\bullet}$ must be located predominantly on P_{D1} because it is closest to the tyrosine, Tyr_Z in D1, and because it has been shown that Tyr_Z acts as the immediate electron donor to $P680^{+\bullet}$ (Gerken et al. 1987, 1988). Therefore the P_{D1}-Ch_{D1}-$Pheo_{D1}$-Q_A branch is the one active in electron transfer.

In a much debated new model for the mechanism of water oxidation developed by the late Jerry Babcock and colleagues (Tommos and Babcock 2000) a key point is the direct hydrogen atom abstraction from the water bound to the Mn cluster realized by the oxidized tyrosine Tyr_Z radical in each turnover. The edge-to-edge distance between the keto-oxygen of Tyr_Z and the Mn cluster is 7 Å (Figure 4). This distance is too large for such a hydrogen abstraction. Hydrogen abstraction via a proton-coupled electron transfer or a water pipeline between the cluster and Tyr_Z may be possible. But, according to the Babcock model, the resulting stoichiometry of the proton release from the two substrate water must be 1:1:1:1 per O_2 evolution during the stepwise extraction of four electrons from the water-oxidizing Mn cluster (see also Renger 2003, this issue). However, this pattern has not been measured: net charge oscillations observed by specific electrochromic absorption changes are indicating the H^+ release from the water-oxidizing catalytic center (Saygin and Witt 1985; Kretschmann et al. 1996). With this method a stoichiometry of 1:0:1:2 was observed. Furthermore, the H^+ pattern of 1:0:1:2 was independently obtained by direct glass electrode measurements of the pH-independent H^+ release from the catalytic center into the medium by use of *crystallizable* PS II material (Schlodder and Witt 1999).

For the first time, information on the position, size and shape of the Mn cluster, the inner sanctum of photosynthesis, has been obtained. The dimensions of its electron density, which bulges in three directions, are 6.8 Å × 4.9 Å × 3.3 Å (Figure 4). The long axis points towards the lumen and is tilted by ∼23° against the membrane plane. Three Mn atoms were assigned to the three bulges, the fourth Mn was assigned to the density remaining near the center. The resulting Mn-topography resembles a distorted Y shape with inter-atomic distances of ∼3 Å. Verification that the density is due to the contribution of manganese was obtained by collecting anomalous diffraction data with

Figure 5. Clockwise from top left: Ingrid Witt, Petra Fromme, Dörte DiFiore, and Athina Zouni of the Max-Volmer-Institute and the author's team who paved the way from protein growing, isolation, and purification to crystallization of PS I and PS II (see text).

X-ray wavelength of the Mn-edge. Many different structural models of the Mn cluster are discussed in the literature as possible candidates for catalyzing water oxidation. In comparison with the here elucidated size and form of the cluster only very few models remain for a closer discussion. The model with two separate Mn-dimers based on ESR analysis (Smith and Pace 1996) as well as the well known C-shaped cluster based on EXAFS measurements (Yachandra et al. 1996) are not supported by the result obtained here. A stronger improvement of structural information about the Mn cluster by EXAFS measurements is expected from the collection of data sets on single crystals in dependence on their orientation; this work has been started by the Max-Volmer-Laboratorium in cooperation with the Berkeley group.

Important for the understanding of the mechanism of the Mn cluster is the knowledge of its immediate environment. According to mutational studies different amino acid residues have been characterized which may provide ligands to the Mn cluster (reviewed in Debus 2001). Regions close enough to provide coordination with the Mn cluster have been localized by helices, β-sheet and loops of the protein backbone of the C-terminus of the D1 subunit completely surrounding the Mn cluster (Zouni et al. 2001b). Thus, with the direct identification of side chains of amino acid residues – possibly already obtained by a small improvement of the resolution – the binding pocket of the cluster should become visible. Ca^{++} ion is a cofactor of water oxidation. *Inter alia*, it is discussed to be a member of the cluster or located in its vicinity. The more detailed structure should also resolve this uncertainty.

At the lumenal side of the RC domain in cyanobacteria the membrane extrinsic subunit Cyt *c*-550 (PbsV) with an unknown redox role, and the main part of the Mn-stabilizing 33 kDa (PsbO) subunit with a tunnel-like β-barrel structure, were identified. Recently, also, the expected 12 kD (PsbU) subunit has been located between the other two extrinsic subunits at the 'bottom' of the extrinsic domain (manuscript submitted).

Implication of the PS II structure on the mechanism of the transmembrane charge separation

With respect to the arrangement of the helices and the central RC chlorins of PS II, there exists an overall symmetry with the RC of purple bacteria. The hope that with elucidation of the PS II structure also fascinating structural peculiarities of the electron transfer chain become visible which explain the unique oxidation potential of P680, necessary to drive water cleavage in the Mn cluster, has not been realized. However, by closer inspection of tiny changes in the ETC structure important features of the nature of the primary electron donors, the oxidation potentials of the cofactors as well as mechanistical perspectives become visible (Witt et al. 2001).

The center-to-center distance of the first pair P_{D1}/P_{D2} assigned to P680 is 10 Å, and, between the ring planes 5 Å (see Figure 4). This indicates a rather weak excitonic coupling of ca. $100\,cm^{-1}$ between P_{D1} and P_{D2} and thus the latter cannot be regarded as a 'special pair.' This is a striking difference compared with P700 of PS I and P870/P960 of purple bacteria which are real dimers. In PS I the corresponding distances are, in Å, 6.3/3.6 and in purple bacteria (*Rb. sphaeroides*) 7.5/3.5. Note that with respect to the question whether the Chls of a pair have to be regarded functionally as a dimer or more as two monomeric Chls, depends apart from the cited distances between both also on their relative orientation and their transition-dipole moments and environment.

The distance between the following four chlorins of the ETC in PS II is also ∼10 Å. Therefore, these cofactors can be regarded as an ensemble of six weakly coupled chlorins, which allows the excited state to be distributed according to the Boltzmann law over all six chlorins. This is in line with the suggestion of a multimer model of the ETC in PS II (Durrant et al. 1995). Due to the weak coupling of the chlorins there is almost no spectral separation between them. Therefore, the absorption bands are largely overlapping and centered between ∼670 and 680 nm. P680 is only weakly red-shifted with ∼10 nm from the maximum of the overall antenna absorption spectrum in contrast to the shift of P700 with ∼30 nm in PS I and of P870 with ∼100 nm in purple bacteria. The antenna system can therefore provide in PS II each of the chlorins with excitation energy followed by transfer between them. This makes the RC of PS II a weak trap for excitation energy; the time for trapping the exciton by P680 becomes thereby relatively long.

Now, the key question arises, which of the chlorins acts as a primary electron donor. P_{D1} is expected to have an oxidation potential of $\geq$1.1 V (Jursinic and Govindjee 1977; Klimov and Krasnovskii 1981) in order to be capable of water oxidation. The center-to-

center distance of P_{D1} is 9.8 Å from Chl_{D1} but 12.4 Å from Tyr_Z. To prevent at this narrow spacing an oxidation of Chl_{D1} by P^+_{D1}, instead of Tyr_Z, it follows the conclusion that the potential of Chl_{D1} must be >1.1 V, for example, 1.2 V. Pheophytin has an oxidation potential of ~1.3–1.4 V already *in vitro*. The potential of P_{D2} should be also >1.1 V, for example, 1.14 V to keep the unpaired electron, that is, the cation of the $P_{D1,D2}$ pair, for oxidation of Tyr_Z predominantly on P_{D1}. This agrees with the observed asymmetrical electron spin distribution of 80:20 for P_{D1} and P_{D2} when P680 is oxidized (Rigby et al. 1994).

The suggested high potential of Chl_{D1} raises the question as to why Chl_{D1} is not the primary electron donor followed by a fast migration of the created positive charge to P_{D1}. It was shown in Diner et al. (2001) by mutation of the His 198 residue of P_{D1} that at 5 K the Q_Y transition energy of Chl_{D1} is clearly lower (~684 nm) than that of P_{D1} (~675 nm) and $Pheo_{D1}$ (~680 nm). Therefore at 5 K, the exciton energy from the antenna system must be trapped exclusively on Chl_{D1}. At <20 K charge separation was observed in the picosecond range with high quantum yield (Wasielewski et al. 1989) which implies that Chl_{D1} is a primary electron donor and the only one at this temperature. This view has been supported also by results of photon echo studies (Prokhorenko and Holzwarth 2000). Independent evidence for this conclusion is based on the observation that at 20 K the Chl triplet state of the electron transfer chain, assumed to be on the same chlorophyll as the primary donor, is located on a monomeric chlorophyll tilted by ~30° with respect to the membrane plane (van Mieghem et al. 1991). But, this is the structure and orientation of Chl_{D1} determined here by the X-ray structure analysis in Figure 4.

At higher temperatures $P_{D1,D2}$ are increasingly excited. This includes also $Pheo_{D1,D2}$ shown by their increase of fluorescence at >70 K (Konermann et al. 1997). At 298 K the excitation energy should be distributed with different probabilities over all six chlorins on the two branches followed by energy transfer between them. The relative locations of the excitation energy gathered on the different chlorins with respect to the total excitation are determined by the Boltzmann distribution law using the values of the lowest electronic transition energy of the chlorins indicated by the maxima of their absorption spectra. The energies of each of the excited three chlorins on the active branch might be used for starting the charge separation. In the first primary step the following two transient radical pair formations might be induced in <1 ps:

$$P^*_{D1} \rightarrow (P^+_{D1} - Chl^-_{D1} - Phe_{D1}) \leftarrow Chl^*_{D1} \rightarrow (P_{D1} - Chl^+_{D1} - Phe^-_{D1}) \leftarrow Phe^*_{D1}$$

Subsequently, the two unstable charged pairs extend spatially into (P^+_{D1} – Chl_{D1} – $Pheo^-_{D1}$) followed by its stabilization in the redox couple (P^+_{D1} – Chl_{D1} – $Pheo_{D1}$ – Q^-_A) (see the section 'The primary electron donor chlorophyll P680 of PS II . . .'). The individual contribution for charge separation by the three excited chlorins would depend not only on the probability to carry the excited state but also on the energy levels of the radical pair states, the kinetics of pair formation and the exciton interaction of the cofactors between the inactive and active branch. This complexity remains to be solved (see also Diner and Rappaport 2002). The predicted two fast primary charge separations have not yet been measured. The first detectable but unstable charged pair is ($P^{+\bullet}_{D1}$ – Chl_{D1} – $Pheo^{-\bullet}_{D1}$) (see Seibert and Wasilewski 2003) followed by the stable state ($P^{+\bullet}_{D1}$ – Chl_{D1} – $Pheo_{D1}$ – $Q^{-\bullet}_A$). The difference spectrum of $P680^{+\bullet}$ – P680 is that measured in the presence of the latter stable state. This spectrum is not only the result of the bleaching at ~675 nm through the formation of the cationic radical state of P_{D1} and – to some extent – of P_{D2} (see above) but also of the electrochromic shift of the ~684 nm absorption band of Chl_{D1} predominantly induced by the charge of $P^{+\bullet}_{D1}$.

A key point in question is how the high oxidation potential of P_{D1} and even the postulated higher one of Chl_{D1} is established. One contribution for an increase of the oxidation potential in PS II nature has been realized by the formation of monomeric primary donors in PS II instead of dimeric ones as realized in PS I and purple bacteria. In a Chl dimer an unpaired π-electron is much more delocalized as in a monomer. Therefore, Chl monomer cations are stronger oxidizing than dimeric cations. The difference is in the order of a few hundred mV as predicted in a range of calculations and experiments. A strong asymmetrical electron spin density established within the macroaromatic cycle of the monomeric Chl as measured *in vivo* on P_{D1} may be also important for the formation of a high oxidation potential (Matysik et al. 2000). Hydrogen bonding between the chlorins and H-atoms of amino acid residues may contribute with a positive shift of 60–100 mV per bond (Allen and Williams 1995) to the potential or the electrostatic influence of positively charged residues in the immediate neighborhood of the Chl (Mulkidjanian 1999). For a Schiff-base

chlorophyll *in vitro* it was shown that its protonation increases the redox potential by 310 mV (Maggiora et al. 1985). Thus, evolution has realized the tuning of high potentials not by visible new structural features, which here became apparent with the outlined structure of PS II, but obviously by tiny changes within the Chl macrocycle and in the microenvironment of the Chl in question, perhaps even only by protonations at the right place.

Einstein might have said: 'I really would be irritated if the Great Man up there had not taken the opportunity to pick the simplest version!' So, we can hope that the above suggestions are perhaps not too far from reality.

Future prospects

For increased insight into the events of PS II the structural resolution has to be improved to be less than 3.6 Å. Provisions have already been made for such a progress with the extensive experiences obtained by the crystallization of the cyanobacterial PS I. There the quality of the crystals was drastically increased by the change from crystallization of the 'salting out' to the 'reverse of salting in' procedure (see the section '3-D crystallization of PS I . . .'). Thus a way is available for significant advances and further information on the refined molecular architecture and reaction sequences of water oxidation in PS II. Together with the outlined 2.5 Å PS I structure, these results will be the basis for an improved understanding of the mechanism of the conversion of sunlight into biochemical energy and O_2 supply from H_2O that makes life possible on our planet.

Acknowledgments

The structures of the photosystems presented here are based on the creative activity of the authors named above and in the references who presented important results obtained in various fields ranging from physical methodological advances to photochemistry, electro- and protein-chemistry and from crystallization procedures to electron- and X-ray crystallography. I would like to express my gratitude to all these colleagues and coworkers whose contributions, cooperations and joint efforts during the last 40 years led to the elucidation of the architecture of the two photosystems driving the photosynthetic machinery.

The X-ray structural analysis of the PS I and PS II crystals was performed in a long-term collaboration for the last 15 years with Professor Wolfram Saenger and Dr Norbert Krauß of the Freie Universität Berlin and their coworkers. The work has been funded by the Deutsche Forschungsgemeinschaft each year from 1952 until now and since 1985 also by the Fonds der Chemischen Industrie. I am very grateful to John Allen, Govindjee, Norbert Krauß, and Eberhard Schlodder for the critical reading of the manuscript and very helpful comments. This article was written upon invitation by Govindjee. The paper was edited by John F. Allen.

References

Adir N (1998) Crystallization of the reaction center of photosystem II. In: Garab G (ed) Photosynthesis: Mechanisms and Effects, Vol II, pp 945–948. Kluwer Academic Publishers, Dordrecht, The Netherlands

Adir N, Zer H, Shochat S and Ohad I (2003) Photoinhibition – a historical perspective. Photosynth Res 76: 343–370

Allen JP (2004) My daily constitutional in Martinsried. Photosynth Res 80: 157–163 (this issue)

Allen JP and Williams JC (1995) Relationship between the oxidation potential of the bacteriochlorophyll dimer and electron transfer in photosynthetic reaction centers. J Bioenerg Biomembr 27: 275–283

Barber J (2004) Engine of life and big bang of evolution: a personal perspective. Photosynth Res 80: 137–155 (this issue)

Barry BA, Boener RJ and Paula IC (1994) The use of cyanobacteria in the study of the structure and function of photosystem II. In: Bryant DA (ed) The Molecular Biology of Cyanobacteria, pp 217–257. Kluwer Academic Publishers, Dordrecht, The Netherlands

Bassham JA (2003) Mapping the carbon reduction cycle: a personal retrospective. Photosynth Res 76: 35–52

Benson AA (2002) Following the path of carbon in photosynthesis: a personal story. Photosynth Res 73: 29–49

Bittl R, Zech SG, Fromme P, Witt HT and Lubitz W (1997) Pulsed EPR structure analysis of Photosystem I single crystals: localization of the phylloquinone acceptor. Biochemistry 36: 12001–12004

Boekema EJ, Dekker JP, van Heel MG, Rögner M, Saenger W, Witt I and Witt HT (1987) Evidence for a trimeric organization of the Photosystem I complex from the thermophilic cyanobacterium *Synechococcus* sp. FEBS Lett 217: 283–286

Bouges-Bocquet B (1973) Electron transfer between two photosystems in spinach chloroplasts. Biochim Biophys Acta 314: 250–256

Brettel K, Sétif P and Mathis P (1986) Flash-induced absorption changes in Photosystem I at low temperature: evidence that the electron acceptor A_1 is vitamin K_1. FEBS Lett 203: 220–224

Buchwald HE and Rüppel H (1968) Suppression of disturbing light signals in rapid flash kinetic measurements. Nature 220: 5758

Clayton RK (2002) Research on photosynthetic reaction centers from 1932–1987. Photosynth Res 73: 63–71

Clayton RK and Straley SC (1970) An optical absorption change that could be due to reduction of the primary photochemical

electron acceptor in photosynthetic reaction centers. Biochem Biophys Res Commun 39: 1114–1119

Crofts AR (2004) The Q-cycle – a personal perspective. Photosynth Res 80: 223–243 (this issue)

Debus R (2001) Amino acid residues that modulate the properties of tyrosine Y_Z and the manganese cluster in the water oxidizing complex of Photosystem II. Biochim Biophys Acta 1503: 164–186

Deisenhofer J, Epp O, Miki K, Huber R and Michel H (1985) Structure of the protein subunits in photosynthetic reaction centers of *Rhodopseudomonas viridis* at 3 Å resolution. Nature 318: 618–624

Dekker JP and van Grondelle R (2000) Primary charge separation in Photosystem II. Photosynth Res 63: 195–208

Dekker JP, Boekema EJ, Witt HT and Rögner M (1988) Refined purification and further characterization of oxygen evolving and Tris-treated Photosystem II particles from the thermophilic cyanobacterium *Synechococcus* sp. Biochim Biophys Acta 936: 307–318

Diner BA and Rappaport F (2002) Structure, dynamics, and energetics of the primary photochemistry of Photosystem II of oxygenic photosynthesis. Annu Rev Plant Biol 53: 551–580

Diner BA, Schlodder E, Nixon PJ, Coleman WJ, Rappaport F, Lavergne J, Vermaas WFJ and Chisholm DA (2001) Site-directed mutations at D1-His198 and D2-His197 of Photosystem II in *Synechocystis* PCC 6803: sites of primary charge separation and cation and triplet stabilization. Biochemistry 40: 9265–9281

Döring G, Stiehl HH and Witt HT (1967) A second chlorophyll reaction in the electron chain of photosynthesis – registration by the repetitive excitation technique. Z Naturforsch 22b: 639–644

Döring G, Bailey JL, Kreutz W, Weikard J and Witt HT (1968a) The action of two chlorophyll-a_I molecules in light reaction I of photosynthesis. Naturwissenschaften 55: 219–224

Döring G, Bailey JL, Kreutz W and Witt HT (1968b) The active chlorophyll-a_{II} in light reaction II of photosynthesis. Naturwissenschaften 55: 219–224

Döring G, Renger G, Vater J and Witt HT (1969) Properties of the photoactive chlorophyll-a_{II} in photosynthesis. Z Naturforsch 24b: 1139–1143

Durrant JR, Klug DR, Kwa SLS, von Grondelle R, Porter G and Dekker JP (1995) A multimer model for P680, the primary electron donor of Photosystem II. Proc Natl Acad Sci USA 92: 4798–4802

Duysens LNM and Sweers HE (1963) Mechanism of two photochemical reactions in algae as studied by means of fluorescence. In: Japanese Society of Plant Physiologists (eds) Studies in Microalgae and Photosynthetic Bacteria, pp 353–372. University of Tokyo Press, Tokyo

Duysens LNM, Amesz J and Kamp BM (1961) Two photochemical systems in photosynthesis. Nature 190: 510–511

Eijekelhoff E and Dekker JP (1995) Determination of the pigment stoichiometry of the photochemical reaction center of Photosystem II. Biochim Biophys Acta 1231: 21–28

Emerson R and Arnold W (1932) A separation of the reactions in photosynthesis by means of intermittent light. J Gen Physiol 15: 391–420

Emerson R, Chalmers R and Cederstrand C (1957) Some factors influencing the long-wave limit of photosynthesis. Proc Natl Acad Sci USA 43: 133–143

Emrich HM, Junge W and Witt HT (1969) Further evidence for an optical response of chloroplast bulk pigments to a light-induced electrical field in photosynthesis. Z Naturforsch 24b: 1144–1146

Ford RC and Holzenburg A (1988) Investigation of the structure of trimeric and monomeric Photosystem I reaction center complexes. EMBO J 7: 2287–2293

Ford RC, Picot D and Garavito RM (1987) Crystallization of the Photosystem I reaction center. EMBO J 6: 1581–1586

Fromme P and Witt HT (1998) Improved isolation and crystallization of Photosystem I for structural analysis. Biochim Biophys Acta 1365: 175–184

Fromme P and Mathis P (2004) Unraveling the Photosystem I reaction center: a history, or the sum of many efforts. Photosynth Res 80: 109–124 (this issue)

Gerken S, Brettel K, Schlodder E and Witt HT (1987) Direct observation of the immediate electron donor to chlorophyll a_{II}^+ ($P680^+$) in oxygen-evolving Photosystem II complexes. Resolution of nanosecond kinetics in the UV. FEBS Lett 223: 376–380

Gerken S, Dekker JP, Schlodder E and Witt HT (1989) Studies on the multiphasic charge recombination between chlorophyll a_{II}^+ and plastoquinone Q_A^- in PS II complexes. UV difference spectrum of Chl a_{II}^+/Chl a_{II}. Biochim Biophys Acta 977: 52–61

Golbeck JH (1994) The structure of Photosystem I. Curr Opin Struct Biol 3: 508–514

Govindjee, Ichimura S, Cederstrand C and Rabinowitch E (1960) Effect of combining far-red light with shorter wave light on the excitation of fluorescence in *Chlorella*. Arch Biochem Biophys 89: 322–323

Hankamer B, Morris EP and Barber J (1999) Revealing the structure of the oxygen-evolving core dimer of PS II by cryoelectron crystallography. Nature Struct Biol 6: 560–564

Hankamer B, Morris EP, Nield J, Gerle Ch and Barber J (2001) Three-dimensional structure of the Photosystem II core dimer of higher plants determined by electron microscopy. J Struct Biol 135: 262–269

Hauska G (2004) The isolation of a functional cytochrome b_6f complex: from lucky encounter to rewarding experiences. Photosynth Res 80: 277–291 (this issue)

Hauska G, Schütz M and Büttner M (1996) The cyt D_6f complex-composition, structure and function. In: Ort DR and Yokum CF (eds) Oxygenic Photosynthesis, pp 377–398. Kluwer Academic Publishers, Dordrecht, The Netherlands

Hill R and Bendall F (1960) Function of two cytochrome components in chloroplasts: a working hypothesis. Nature 1186: 136–137

Hladik J and Sofrova D (1991) Does the trimeric form of the Photosystem I reaction center of cyanobacteria *in vivo* exist? Photosynth Res 29: 171–175

Hofbauer W, Zouni A, Bittl R, Jern J, Orth P, Lendzian F, Fromme P, Witt HT and Lubitz W (2001) Photosystem II single crystals studied by EPR spectroscopy at 94 GHz: the tyrosine radical Y_D^*. Proc Natl Acad Sci USA 98: 6623–6628

Jackson JB and Crofts AB (1969) The high energy state in chromatophores from *Rhodospeudomonas sphaeroides*. FEBS Lett 4: 185–189

Jagendorf AT (2002) Photophosphorylation and chemiosmotic perspective. Photosynth Res 73: 233–241

Joliot P and Joliot A (1999) *In vivo* analysis of the electron transfer within PS I: are the two phylloquinones involved? Biochemistry 38: 11130–11136

Joliot P and Kok B (1975) Oxygen evolution in photosynthesis. In: Govindjee (ed) Bioenergetic of Photosynthesis, pp 387–412. Academic Press, New York

Jordan P, Fromme P, Klukas O, Witt HT, Saenger W and Krauß N (2001) Three-dimensional structure of cyanobacterial Photosystem I at 2.5 Å resolution. Nature 411: 909–917

Junge W and Witt HT (1968) On the ion transport system of photosynthesis – investigations on a molecular level. Z Naturforsch 23b: 244–254

Jursinic P and Govindjee (1977) Temperature dependence of delayed light emission in the 6 to 340 μs range after a single flash in chloroplasts. Photochem Photobiol 26: 617–628

Käß H, Fromme P, Witt HT and Lubitz W (2001) Orientation and electronic structure of the oxidized primary donor $P_{700}^{+\cdot}$ in Photosystem I: a single crystal EPR and ENDOR study. J Phys Chem 105: 1225–1239

Kamen MD (1963) Primary Processes in Photosynthesis. Advanced Biochemistry. Academic Press, New York

Kamlowski A, Zech S, Fromme P, Bittl R, Lubitz W, Witt HT and Stehlik D (1998) The radical pair state $P_{700}^{+\cdot}$ $A_1^{-\cdot}$ in Photosystem I single crystals: orientation dependence of the transient spin-polarized EPR spectra. J Phys Chem B 102: 8266–8277

Kautsky H, Appel W and Amann H (1960) Chlorophyllfluoreszenz und Kohlensäureassimilation. XIII. Mitteilung. Die Fluoreszenzkurve und die Photochemie der Pflanze. Biochem Z 332: 277–292

Ke B (2001) Photosynthesis: Photobiochemistry and Photobiophysics. Kluwer Academic Publishers, Dordrecht, The Netherlands

Klimov VV (2003) Discovery of pheophytin function in the photosynthetic energy conversion as the primary electron acceptor of Photosystem II. Photosynth Res 76: 247–253

Klimov VV and Krasnovskii AA (1981) Pheophytin as the primary electron acceptor in Photosystem II reaction center. Photosynthetica 15: 592–609

Kok B (1956) On the reversible absorption change at 705 mμ in photosynthetic organisms. Biochim Biophys Acta 22: 399–401

Kok B (1961) Partial purification and determination of oxidation reduction potential of the photosynthetic chlorophyll complex absorbing at 700 mμ. Biochim Biophys Acta 48: 527–533

Kok B and Hoch G (1961) Spectral changes in photosynthesis. In: McElroy WD and Glass B (eds) Light and Life, pp 397–416. Johns Hopkins University Press, Baltimore, Maryland

Konermann L, Yruela I and Holzwarth AR (1997) Pigment assignment in the absorption spectrum of the Photosystem II reaction center by site-selection fluorescence spectroscopy. Biochemistry 36: 7450–7498

Krauß N, Hinrichs W, Witt I, Fromme P, Pritzkow W, Dauter Z, Betzel Ch, Wilson KS, Witt HT and Saenger W (1993) Three-dimensional structure of System I of photosynthesis at 6 Å resolution. Nature 361: 326–331

Krauß N, Schubert W-D, Klukas O, Fromme P, Witt HT and Saenger W (1996) Photosystem I at 4 Å resolution represents the first structural model of a joint photosynthetic reaction center and core antenna system. Nat Struct Biol 3: 965–973

Kretschmann H, Schlodder E and Witt HT (1996) Net charge oscillation and proton release during water oxidation in photosynthesis. An electrochromic band shift study at pH 5.5–7.0. Biochim Biophys Acta 1274: 1–8

Kuhl H, Rögner M, van Breemn JFL and Boekema EJ (1999) Localization of cyanobacterial Photosystem II donor-side subunits by electron microscopy and the supramolecular organization of Photosystem II in the thylakoid membrane. Eur J Biochem 266: 453–459

Kuhl H, Kruip J, Seidler A, Krieger-Liszkay A, Bünker M, Bald D, Scheidig AJ and Rögner M (2000) Towards structural determination of the water-splitting enzyme. Purification, crystallization, and preliminary crystallographic studies of Photosystem II from a thermophilic cyanobacterium. J Biol Chem 275: 20652–20659

Lubitz W (2002) Pulse EPR and ENDOR studies of light-induced radicals and triplet states in Photosystem II of oxygenic photosynthesis. Phys Chem Phys 4: 5539–5545

Maggiora LL, Petke JD, Gopal D, Iwamoto RT and Maggiora GM (1985) Experimental and theoretical studies of Schiff base chlorophylls. Photochem Photobiol 42: 69–75

Malkin R (1986) On the function of two vitamin K_1 molecules in the PS I–electron acceptor complex. FEBS Lett 208: 343–346

Matysik J, Gast P, van Gorkom HJ, Hoff AJ and de Groot HJM (2000) Photochemically induced nuclear spin polarization in reaction centers of Photosystem II observed by ^{13}C-solid-state NMR reveals a strongly asymmetric electronic structure of the $P_{680}^{+\cdot}$ primary donor chlorophyll. PNAS 97: 9865–9870

Michel H and Deisenhofer J (1988) Relevance of the photosynthetic reaction center from purple bacteria to the structure of Photosystem II. Biochemistry 27: 17

Mitchell P (1961) Coupling of phosphorylation to electron and proton transfer by a chemiosmotic type of mechanisms. Nature 191: 144–148

Mühlenhoff U, Haehnel W, Witt HT and Herrmann RG (1993) Genes encoding eleven subunits of Photosystem I from the thermophilic cyanobacterium *Synechococcus* sp. 192. Gene 127: 73–78

Mulkidjanian AY (1999) Photosystem II of green plants: on the possible role of retarded protonic relaxation in water oxidation. Biochim Biophys Acta 1410: 1–6

Nelson N and Ben-Shem A (2002) Photosystem I reaction center: past and future. Photosynth Res 73: 193–206

Nield J, Orlova EV, Morris EP, Gowen B, van Heel M and Barber J (2000) 3D map of the plant Photosystem II supercomplex obtained by cryoelectron microscopy and single particle analysis. Nat Struct Biol 7: 44–47

Norris JR, Uphaus RA, Crespi HL and Katz JJ (1971) Electron spin resonance of chlorophyll and the origin of signal I in photosynthesis. Proc Natl Acad Sci USA 68: 625–628

Parson WW (2003) Electron donors and acceptors in the initial steps of photosynthesis in purple bacteria: a personal account. Photosynth Res 76: 81–92

Prokhorenko VI, Holzwarth AR (2000) Primary processes and structure of Photosystem II reaction center: a photon echo study. J Phys Chem 104: 11563–11578

Renger G (2003) Apparatus and mechanism of photosynthetic oxygen evolution: a personal retrospective. Photosynth Res 76: 269–288

Rhee K-H (2001) Photosystem II: the solid structural era. Ann Rev Biophys Biomol Struct 30: 307–328

Rhee K-H, Morris EP, Zheleva D, Hankamer B, Kühlbrandt W and Barber J (1997) Two-dimensional structure of plant system II at 8 Å resolution. Nature 389: 522–526

Rhee K-H, Morris EP, Barber J and Kühlbrandt W (1998) Three-dimensional structure of the plant Photosystem II reaction center at 8 Å resolution. Nature 396: 283–286

Rigby SEJ, Nugent JHA and O'Malley PJ (1994) ENDOR and special triple resonance studies of chlorophyll cation radicals in Photosystem 2. Biochemistry 33: 10043–10050

Rögner M, Dekker JP, Boekema EJ and Witt HT (1987) Size, shape and mass of the oxygen-evolving Photosystem II complex from the thermophilic cyanobacterium *Synechococcus* sp. FEBS Lett 219: 207–211

Rögner M, Mühlenhoff U, Boekema EJ and Witt HT (1990) Mono-, di- and trimeric PS I reaction center complexes isolated from the

thermophilic cyanobacterium *Synechococcus* sp. Size, shape and activity. Biochim Biophys Acta 1015: 415–424

Rüppel H and Witt HT (1969) Measurements of fast reactions by single and repetitive excitation with pulses of electromagnetic radiation. In: Kustin K (ed) Methods in Enzymology, pp 317–379. Academic Press, New York

Ruffle SV, Donnelly D, Blundell TL and Nugent JHA (1992) A three-dimensional model of the Photosystem II reaction center of *Pisum sativum*. Photosynth Res 34: 287–300

Rumberg B (1964) Die Eigenschaften des Reaktionszyklus von Chl-a_I-430-703. Z Naturforsch 19b: 707–716

Rumberg B and Witt HT (1964) Die Photooxidation von Chlorophyll-a_I-430-703. Naturforsch 19b: 693–707

Saygin Ö and Witt HT (1985) Evidence for the electrochromic identification of the change of charges in the four oxidation steps of the photoinduced water cleavage in photosynthesis. FEBS Lett 187: 224–226

Schatz GH and Witt HT (1984a) Extraction and characterization of oxygen-evolving Photosystem II complexes from a thermophilic cyanobacterium *Synechococcus* sp. Photobiochem Photobiophys 7: 1–4

Schatz GH and Witt HT (1984b) Characterization of electron transport in oxygen-evolving Photosystem II complexes from a thermophilic cyanobacterium *Synechococcus* sp. Photobiochem Photobiophys 7: 77–89

Schliephake W, Junge W and Witt HT (1968) Correlation between field formation, proton translocation and the light reactions in photosynthesis. Z Naturforsch 23b: 1571–1578

Schlodder E and Witt HT (1999) Stoichiometry of proton release from the catalytic center in photosynthetic water oxidation. J Biol Chem 274: 30387–30392

Schmidt S, Reich R and Witt HT (1971) Electrochromism of chlorophylls and carotenoids in multilayers and in chloroplasts. Naturwissenschaften 58: 414

Schmidt S, Reich R and Witt HT (1972) Electrochromic measurements *in vitro* as a test for the interpretation of field-indicating absorption changes in photosynthesis. In: Forti G, Avron M and Melandri A (eds) Proceedings Second International Congress on Photosynthesis Research, Stresa, Italy, 1971, pp 1087–1095. Dr W. Junk Publishers, The Hague, The Netherlands

Schubert W-D, Klukas O, Krauß N, Saenger W, Fromme P and Witt HT (1997) Photosystem I of *Synechococcus elongatus* at 4 Å resolution: comprehensive structure analysis. J Mol Biol 272: 741–769

Schubert W-D, Klukas O, Saenger W, Witt HT, Fromme P and Krauß N (1998) A common ancestor for oxygenic and anoxygenic photosynthetic systems: a comparison based on the structural model of Photosystem I. J Mol Biol 280: 297–314

Seibert M and Wasilewski M (2003) The isolated Photosystem II reaction center: first attempts to directly measure the kinetics of primary charge separation. Photosynth Res 76: 263–268

Shen J-R and Kamiya N (2000) Crystallization and the crystal properties of the oxygen-evolving Photosystem II from *Synechococcus vulcanus*. Biochemistry 39: 14739–14744

Shin M (2004) How is ferredoxin-NADP reductase involved in the NADP photoreduction of chloroplasts? Photosynth Res 80: 307–313 (this issue)

Shuvalov VA and Klimov VV (1976) The primary photoreaction in the complex cytochrome P890-P760 (bacteriopheophytin 760) of *Chromatium minutissimum* at low redox potentials. Biochim Biophys Acta 440: 587–599

Slooten L (1972) Electron acceptors in reaction center preparations from photosynthetic bacteria. Biochim Biophys Acta 275: 208–218

Smith PJ and Pace RJ (1996) Evidence for two forms of the $g = 4.1$ signal in the S_2 state of Photosystem II. Two magnetically isolated manganese dimers. Biochim Biophys Acta 1275: 213–220

Stiehl HH and Witt HT (1968) Die kurzzeitigen ultravioletten Differenzspektren bei der Photosynthese. Z Naturforsch 23b: 220–224

Stiehl HH and Witt HT (1969) Quantitative treatment of the function of plastoquinone in photosynthesis. Z Naturforsch 24b: 1588–1598

Svensson B, Etchebest C, Tuffery P, van Kann PJ, Smith J and Styring S (1996) A model for the Photosystem II reaction center core including the structure of the primary donor P680. Biochemistry 35: 14486–14502

Tiemann R, Renger G, Gräber P and Witt HT (1979) The plastoquinone pool as possible hydrogen pump in photosynthesis. Biochim Biophys Acta 546: 498–519

Tommos C and Babcock GT (2000) Proton and hydrogen currents in photosynthetic water oxidation. Biochim Biophys Acta 1458: 199–219

Trebst A (1985) The topology of the plastoquinone and herbicide binding peptides of Photosystem II in the thylakoid membrane. Z Naturforsch 41c: 240–245

van Gorkom HJ (1974) Identification of the reduced primary electron acceptor of Photosystem II as a bound semiquinone anion. Biochim Biophys Acta 347: 439–442

van Mieghem FJE, Satoh K and Rutherford AW (1991) A chlorophyll tilted 30° relative to the membrane in the photosystem II reaction center. Biochim Biophys Acta 1058: 379–385

Vasmel H and Amesz J (1983) Photoreduction of menaquinone in reaction centers of green photosynthetic bacterium *Chloroflexus aurantiacus*. Biochim Biophys Acta 724: 118–121

Velthuys BR and Amesz J (1974) Charge accumulation and the reducing side of Photosystem 2 of photosynthesis. Biochim Biophys Acta 333: 85–94

Vermaas WJF, Styring S, Schröder WP and Andersson B (1993) Photosynthetic water oxidation: the protein framework. Photosynth Res 38: 249–263

Vermeglio A (2002) The two-electron gate in photosynthetic bacteria. Photosynth Res 73: 83–86

Wasielewski MR, Johnson DG, Govindjee, Preston C and Seibert M (1989) Determination of the primary charge separation rate in Photosystem II reaction centers at 15 K. Photosynth Res 22: 89–99

Watanabe T, Kobayashi M, Hongu A, Nakazato M, Hiyama T and Murata N (1985) Evidence that a chlorophyll a' dimer constitutes the photochemical reaction center I (P700) in photosynthetic apparatus. FEBS Lett 191: 252–256

Witt HT (1967) A. Direct measurements of reactions in the 10^{-1} to 10^{-8} second range by single and repetitive excitations with pulses of electromagnetic waves (flashes, microwaves, giant laser pulses). B. On the analysis of photosynthesis by pulse techniques in the 10^{-1} to 10^{-8} second range. In: Claesson S (ed) Fast Reactions and Primary Processes in Chemical Kinetics (Nobel Symposium V), (A) pp 81–97 and (B) pp 261–316. Almquist and Wiksell, Stockholm

Witt HT (1971) Coupling of quanta, electrons, fields, ions, and phosphorylation in the functional membrane of photosynthesis. Results by pulse spectroscopic methods. Q Rev Biophys 4: 365–477

Witt HT (1979) Energy conversion in the functional membrane of photosynthesis. Analysis by light pulse and electric pulse methods. The central role of the electric field. Biochim Biophys Acta 505: 355–427

Witt HT (1991) Functional mechanism of water splitting photosynthesis. Photosynth Res 29: 55–77

Witt HT (1996a) Primary reactions of oxygenic photosynthesis. Ber Bunsenges Phys Chem 100: 1923–1942

Witt HT (1996b) Structure analysis of single crystals of photosystem I by X-ray, EPR and ENDOR: a short status report. In: Ort DR and Yocum CF (eds) Oxygenic Photosynthesis: the Light Reactions, pp 363–375. Kluwer Academic Publishes, Dordrecht, The Netherlands

Witt K and Wolff Ch (1970) Rise time of the absorption changes of chlorophyll-a_{I} and carotenoids in photosynthesis. Z Naturforsch 25b: 387

Witt HT, Müller A and Rumberg B (1961a) Experimental evidence for the mechanism of photosynthesis. Nature 191: 194–195

Witt HT, Müller A and Rumberg B (1961b) Oxidized cytochrome and chlorophyll in photosynthesis. Nature 192: 967

Witt I, Witt HT, Gerken S, Saenger W, Dekker JP and Rögner M (1987) Crystallization of reaction center I of photosynthesis. Low-concentration crystallization of photoactive protein complexes from the cyanobacterium *Synechococcus* sp. FEBS Lett 221: 260–264

Witt I, Witt HT, DiFiore D, Rögner M, Hinrichs W, Saenger W, Granzin J, Betzel CH and Dauter Z (1988) X-ray characterization of single crystals of the reaction center I of water-splitting photosynthesis. Ber Bunsenges Phys Chem 92: 1503–1506

Witt HT, Krauß N, Hinrichs W, Witt I, Fromme P and Saenger W (1992) Three-dimensional crystals of Photosystem I from *Synechococcus* sp. and X-ray structure analysis at 6 Å resolution. In: Murata N (ed) Research in Photosynthesis, Vol I, pp 521–528. Kluwer Academic Publishers, Dordrecht, The Netherlands

Witt HT, Zouni A, Kern J, Fromme P, Krauß N, Saenger W and Orth P (2001) Crystal structure of Photosystem II and aspects of its function. In: Critchley C (ed) Proceedings of the 12th International Congress on Photosynthesis, Brisbane, Australia, PL-1, pp 1–8. CSIRO, Melbourne, Australia

Wolff Ch and Witt HT (1969) On metastable states of carotenoids in primary events of photosynthesis. Z Naturforsch 240: 1031–1037

Wolff Ch, Buchwald HE, Rüppel H, Witt K and Witt HT (1969) Rise time of the light-induced electrical field across the function membrane of photosynthesis. Z Naturforsch 24b: 1038–1041

Xiong J, Subramaniam S and Govindjee (1996) Modeling of the D1/D2 proteins and cofactors of the Photosystem II reaction center: implications for herbicide and bicarbonate binding. Protein Sci 5: 2054–2073

Yachandra VK, Sauer K and Klein MP (1996) Manganese cluster in photosynthesis: where plants oxidize water to dioxygen. Chem Rev 96: 2927–2950

Zech SG, Hofbauer W, Kamlowski A, Fromme P, Stehlik D, Lubitz W and Bittl R (2000) A structural model for the charge separated state $P_{700}^{+\bullet}A_1^{-\bullet}$ in Photosystem I from the orientation of the magnetic interaction tensors. J Phys Chem B 104: 9728–9739

Zouni A, Lüneberg C, Fromme P, Schubert W-D, Saenger W and Witt HT (1998) Characterization of single crystals of Photosystem II from the thermophilic cyanobacterium *Synechococcus elongatus*. In: Garab G (ed) Photosynthesis: Mechanisms and Effects, Vol II, pp 925–928. Kluwer Academic Publishers, Dordrecht, The Netherlands

Zouni A, Jordan R, Schlodder E, Fromme P and Witt HT (2000) First Photosystem II crystals capable of water oxidation. Biochim Biophys Acta 1457: 103–105

Zouni A, Witt HT, Kern J, Fromme P, Krauß N, Saenger W and Orth P (2001a) Crystal structure of Photosystem II from *Synechococcus elongatus* at 3.8 Å resolution. Nature 409: 739–743

Zouni A, Kern J, Loll B, Fromme P, Witt HT, Orth P, Krauß N, Saenger W and Biesiadka J (2001b) Biochemical characterization and crystal structure of water oxidizing Photosystem II from *Synechococcus elongatus*. In: Critchley C (ed) 12th International Congress on Photosynthesis, Brisbane, Australia, S5-003, pp 1–6. CSIRO, Melbourne, Australia